Desalination 429 (2018) 142–154

Contents lists available at ScienceDirect

Desalination

journal homepage: www.elsevier.com/locate/desal

A novel single-pass reverse osmosis configuration for high-purity water production and low energy consumption in seawater desalination

Jungbin Kim, Seungkwan Hong*

School of Civil, Environmental and Architectural Engineering, Korea University, 145 Anam-ro, Seongbuk-gu, Seoul 02841, Republic of Korea

GRAPHICAL ABSTRACT

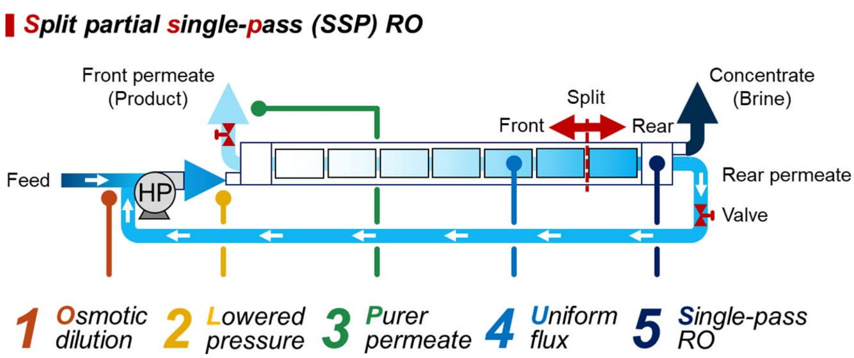

ARTICLE INFO

Keywords:
Reverse osmosis (RO)
Split partial single pass (SSP)
Seawater desalination
Pure permeate
Low energy

ABSTRACT

Seawater reverse osmosis (SWRO) desalination is required to produce high-quality water to meet stricter water standards, which could be satisfied with single-pass RO through the advancement of reverse osmosis (RO) membranes. In this study, a novel single-pass RO configuration was proposed to further improve permeate quality. Split partial single-pass (SSP) RO is a design in which the permeate from the rear RO element(s) in a pressure vessel is blended with the RO feed. This blending resulted in the dilution of the feed, leading to the production of high-quality permeate with lower energy demand. Modeling of the RO process demonstrates that SSP RO had the highest energy efficiency when the permeate from the 7th element (i.e., the last one in the single pass RO configuration) was circulated back and mixed with the feed. For typical SWRO operating conditions, SSP RO was effectively able to improve permeate quality. In fact, SSP RO produced an approximately 15% purer permeate compared to conventional single-pass RO. SSP RO was also always more energy-efficient than the two-pass RO configurations. The economic feasibility of the design was assessed further and the possibility of its practical application explored.

Abbreviations: BP, boost pump; BWRO, brackish water reverse osmosis; CAPEX, capital expenditure; CC, capital cost; CCD, closed circuit desalination; DWEER, dual work exchanger energy recovery; ERD, energy recovery device; FF, flow factor; GSM, golden section method; HID, hybrid RO membrane inter-stage design; HP, high-pressure pump; ISD, internally staged design; OC, operation cost; OPEX, operating expenditure; PRO, pressure retarded osmosis; PV, pressure vessel; PX, pressure exchanger; RO, reverse osmosis; SEC, specific energy consumption; SPSP, split partial second pass; SSP, split partial single pass; SWIP, seawater intake and pretreatment; SWRO, seawater reverse osmosis; TDS, total dissolved solids; UPC, unit product cost; UPW, ultrapure water

* Corresponding author.
E-mail address: skhong21@korea.ac.kr (S. Hong).

https://doi.org/10.1016/j.desal.2017.12.026
Received 27 August 2017; Received in revised form 7 December 2017; Accepted 7 December 2017
0011-9164/ © 2017 Elsevier B.V. All rights reserved.

1. Introduction

To address the challenges of water scarcity arising from global climate change, seawater desalination is a promising method for producing freshwater from the ocean. This is primarily achieved through membrane-based or thermal-based desalination. Following the development of energy recovery devices (ERDs), reverse osmosis (RO)-based processes have become increasingly common worldwide in the pursuit of energy-efficient desalination. Most seawater reverse osmosis (SWRO) desalination plants employ single-pass (or single-stage) RO [1]. Single-pass RO is a compact configuration but the quality of the final product is inferior. To satisfy the growing demand for high-purity water, an additional step is required to treat the water produced by single-pass RO. Therefore, more recent SWRO desalination plants adopt a two-pass RO design.

Two-pass (or full two-pass) RO is a system in which the first-pass RO permeate is treated in its entirety at the second-pass RO. However, extra mineral recovery generally follows for water production. A common example of a two-pass RO configuration is partial two-pass (or partial second-pass) RO, in which a portion of the first-pass RO permeate bypasses the second pass and subsequently mixes with the permeate derived from this second pass. A more advanced partial pass design, split partial second-pass (SPSP) RO, has been applied in SWRO desalination plants. This design also adopts second-pass RO, but in this case, the first-pass RO permeate is collected at the front and rear of the pressure vessel (PV). The front permeate, which has lower total dissolved solids (TDS), bypasses second-pass RO, while the rear permeate is fed into the second-pass RO system, after which the two streams are blended. RO designs such as these that use second-pass RO improve permeate quality, but extra energy is required to run the additional RO step, which significantly increases the total energy consumption of SWRO plants.

The RO process accounts for most of the energy requirements for SWRO desalination plants. According to previous studies, RO systems with an ERD (excluding pretreatment and posttreatment) consume 2.4 to 3.8 kWh/m^3 depending on the SWRO plant in question (Table 1) [2–5]. The total specific energy consumption (SEC) of an SWRO plant varies depending on the operating conditions (e.g., feed and product salinity, water temperature), the type of ERD, and the RO configuration, and this has typically been found to range between 3.5 and 4.5 kWh/m^3 [6]. However, some SWRO plants have been reported to consume under 3.5 kWh/m^3 [7], which can be explained by the low salinity and high temperature of the feed, by the RO configuration, or by technological advances. Recent studies [8–10] have suggested that energy sources from outside an SWRO plant, such as renewable energy or energy harvested from pressure retarded osmosis (PRO), can reduce SEC. However, the total amount of energy required to operate an RO system remains unchanged. Thus, it is important to adopt a low-energy RO configuration in conjunction with the pursuit of supplemental energy sources.

Since a single-pass design is energy-efficient compared to two-pass designs, single-pass RO is preferred for application if the product quality satisfies the requirement. Single-pass RO also has more advantages over two-pass ROs such as reduced costs and low chemical usage. Recently, the advancement of RO membrane even allows single-pass RO to produce high-quality water. In particular, the high-selective membrane improves the product quality of first-pass RO and therefore additional RO step, such as brackish water reverse osmosis (BWRO), might not be required [11]. In spite of the development of high-performance membranes, a higher product quality is required for single-pass RO in some places where stringent water standards are applied for drinking water, industrial use, or agricultural irrigation (i.e., low boron and chloride concentration) [12]. Therefore, a new single-pass configuration is to be developed beyond conventional single-pass RO with the employment of advanced RO membranes.

To gain the benefits and correct the flaw of single-pass design, this study seeks to develop a new single-pass RO process with low energy requirements that produces permeate of high purity. As a result, split partial single-pass (SSP) RO is developed and proposed in this paper to produce higher-quality product with reduced energy consumption. Similar to SPSP, the first-pass permeate is collected from both sides of the PV in SSP but, rather than using the back permeate as the feed for second-pass RO, it is used to dilute the first-pass RO feed (i.e., the back permeate is fed back into the first-pass RO feed). With the adoption of this SSP RO design, high-purity permeate can be produced using single-pass RO and this also can reduce the SEC and operating costs of SWRO plants when compared to current RO systems that produce water of high purity.

In this paper, the SSP RO process is proposed and developed for the first time for SWRO desalination plants, and the performance and feasibility of the SSP RO design are examined using RO process modeling. The product quality, SEC, and economic benefits are also analyzed in comparison with other RO configurations under various operating conditions to determine the feasibility of SSP RO application.

Table 1
Comparison of the SEC for different SWRO desalination plants. Recent SWRO desalination plants have adopted two-pass RO systems to meet restrictive water standards.

Country	Location	TDS (mg/L)		Temperature (°C)	RO pass configuration	ERD type	SEC (kWh/m^3)		Reference
		Feed	Product				Total	RO system	
Australia	Perth	36,500	< 200[a]	20.2	Partial two pass	PX	3.6	2.4[d]	[2,13]
Israel	Soreq	40,800	< 300[a]	27.0	SPSP	DWEER	< 4.0	2.7[d]	[3,14]
	Hadera	40,700	< 270[a]	22.5	SPSP	PX	4.0	2.7[d]	[3,14,15]
	Ashkelon	40,700	< 80[b]	22.5	SPSP[c]	DWEER	3.9	3.0[d]	[3,16,17]
	Palmachim 1	42,000	< 300[a]	24.5	SPSP	Pelton turbine	3.5	2.9[d]	[3,18–20]
	Palmachim 2					PX		2.7[d]	
Saudi Arabia	Sadara	< 45,000	< 40[b]	26.5	Partial two pass	PX	4.4	3.1[e]	[4]
Singapore	Tuas (Singspring)	31,600	< 250[a]	30.6	Partial two pass	DWEER	4.1	3.1[d]	[3,21,22]
UAE	Fujairah	38,250	< 120[b]	29.0	Partial two pass	Pelton turbine	4.5	3.8[e]	[5]

TDS: total dissolved solids. SPSP: split partial second pass. ERD: energy recovery device. PX: pressure exchanger. DWEER: dual work exchanger energy recovery. SEC: specific energy consumption.
[a] After the remineralization process.
[b] Before the remineralization process.
[c] Additional BWRO passes are adopted to meet boron and chloride concentration standards.
[d] SEC of SWRO-ERD.
[e] SEC of SWRO-ERD and BWRO.

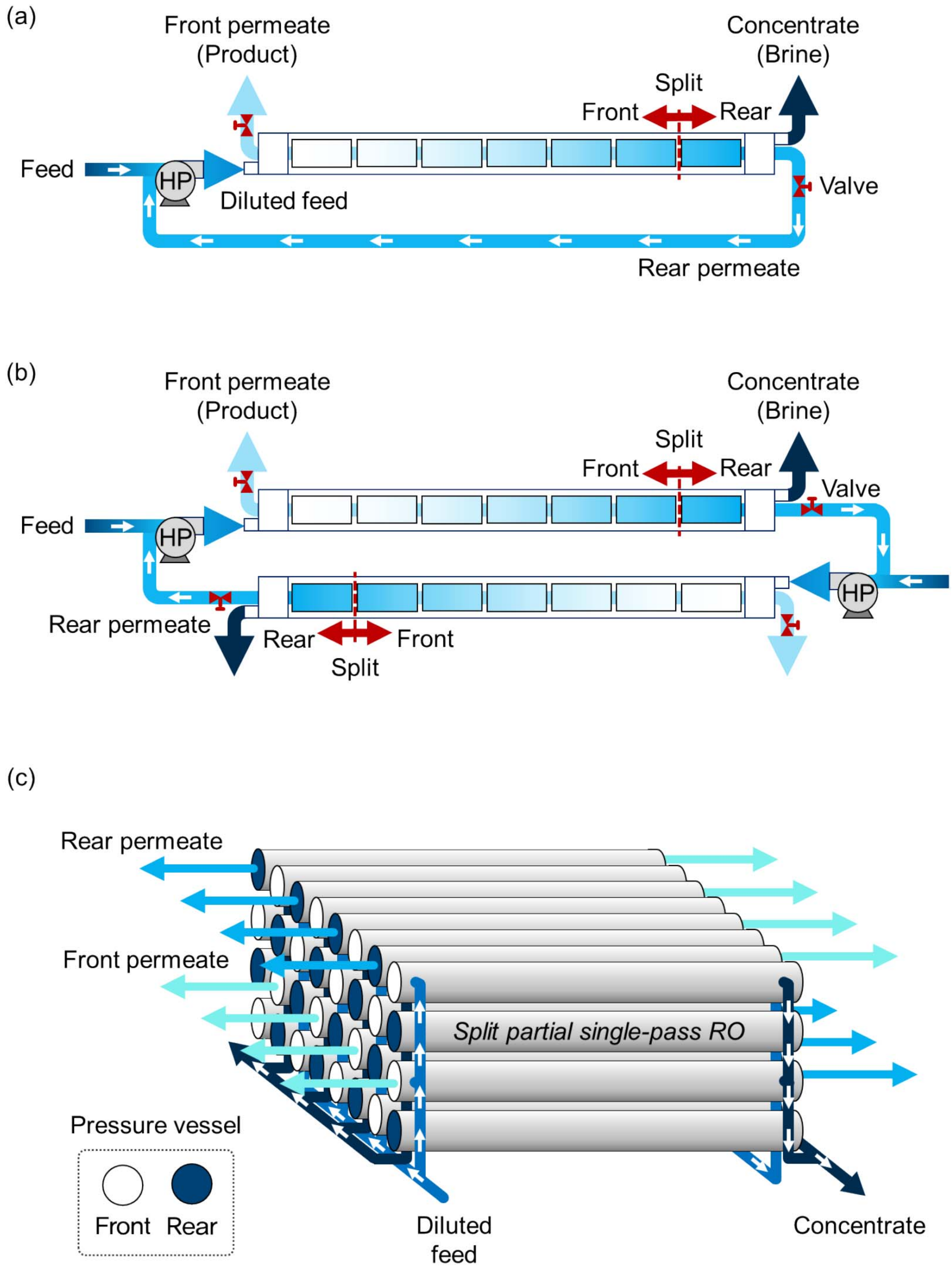

Fig. 1. Schematic design of an SSP RO system for use in SWRO desalination plants. The concept of SSP RO design is illustrated in (a). Practical SSP RO designs for (b) a single unit and (c) a train are proposed to reduce piping costs.

2. Review of RO configurations

2.1. Split partial single-pass RO design

In an RO system, hydraulic pressure is applied on the feed side to produce permeate across the membrane. With the permeate continuously being taken out, the feed becomes more concentrated as it passes through the PV, and thus the TDS of the permeate increases as the feed moves from the front to the rear elements. Although the permeate from the rear elements has a higher TDS than that from the front, it is still significantly purer than the original RO feed. Therefore, if the rear permeate is blended with the RO feed, the feed is diluted and higher quality permeate is produced.

Based on this concept, SSP RO was developed as a novel RO system in which the permeate from the rear RO element(s) is blended with the RO feed. However, the concentrations of the rear permeate and the SWRO feed differ significantly and the mixing of solutions with different concentrations can increase the levels of entropy leading to entropic loss [23,24]. To minimize this energy loss, the rear permeate is blended with the SWRO feed before pressurization, as illustrated in Fig. 1(a). In general, this SSP design may be described as an SPSP design that utilizes single-pass RO but not second-pass RO.

To implement the SSP RO design in SWRO desalination plants, pipelines for the transport of the rear permeate to the SWRO feed are required. This naturally has an economic disadvantage in that it increases the cost of piping. To avoid this, two PVs are operated side by side, forming the unit depicted in Fig. 1(b). Several of these units are grouped together to form the train shown in Fig. 1(c), which has high-

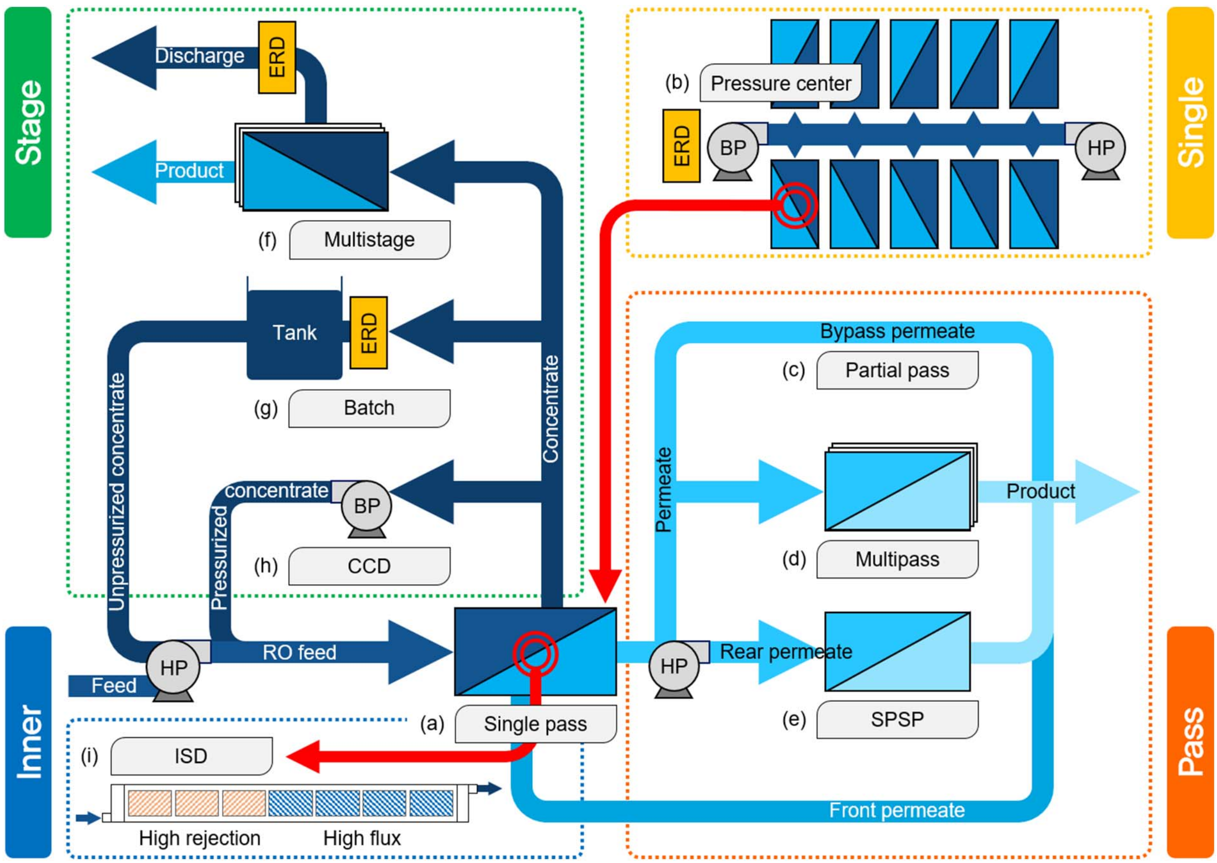

Fig. 2. Schematic diagram of various RO configurations. (a) Single pass, (b) pressure center, (c) partial pass, (d) multipass, (e) SPSP, (f) multistage, (g) batch, (h) CCD, and (i) ISD designs have been combined to satisfy the purpose of the RO process. HP: high-pressure pump. BP: boost pump. ERD: energy recovery device. SPSP: split partial second pass. CCD: closed circuit desalination. ISD: internally staged design.

pressure pumps (HPs) located on each side. The rear permeate is collected and sent to the SWRO feed tank, where the rear permeate and the feed are blended together. The permeate from the front elements is collected and undergoes post treatment.

2.2. RO design innovations

RO is an effective and energy-efficient method for the production of pure water, especially when compared to thermal desalination. However, careful consideration of the RO configuration is required to optimize SWRO performance. Several RO designs have been developed for various purposes, including low-energy desalination and high-quality water production. These configurations can be classified into four groups: single, pass, stage, and inner designs. These RO designs are summarized in Fig. 2 and systematically reviewed in Table 2.

Single-pass (or single-stage) RO is the most common configuration used in seawater desalination because of its simplicity and ease of use. High pressure is applied to the feed and the RO membranes produce permeate from a single pass of the pressurized feed. Any energy remaining in the concentrate is recovered using an ERD and the concentrate is then discharged. A single-pass train design is implemented with a pressure center (or a three-center RO system) in which RO membranes, the HP, and the ERD with boost pump (BP) are combined. This design allows for an increase in the size of pumps leading to an improvement in pump efficiency. In addition, such integrated system can lower energy use when producing varying flows resulting in operational flexibility. With these benefits, the SEC of SWRO plants can be reduced [25].

Pass designs are utilized to improve product quality. In general, the permeate from a previous RO pass is treated again with an additional RO pass. By doing so, the permeate becomes purer. For seawater desalination, more modern SWRO plants typically employ two passes to meet restrictive water quality standards, though they tend to favor the partial two-pass or SPSP RO versions of this design in order to produce freshwater with TDS levels that meet regulatory standards [26–28] while at the same time reducing energy expenditure. The use of more than two passes is uncommon in seawater desalination but this can be observed in industry where ultrapure water (UPW) is required. Triple-pass RO produces permeate of the highest purity [29], but this comes at the expense of additional energy costs.

Unlike pass designs, stage designs are configured so that the concentrate resulting from the previous RO stage is treated again with RO. This design can increase overall system recovery by gaining more product and therefore lowering the SEC of an SWRO plant [30,31], which can be calculated as power consumption divided by the amount of product. However, the fact that the concentrate is used as a feed for the additional RO negatively affects product quality. The increased TDS concentration of the feed solution leads to the production of permeate with high TDS levels. This means that the multistage design is more suitable for the BWRO process. In SWRO plants with two passes, the multistage design is often applied to recover water from the concentrate that results from the BWRO process. The final concentrate of multistaged BWRO is then fed to SWRO feed due to its purity compared to the feed.

Newly developed stage-design concepts include closed circuit desalination (CCD) and batch RO. A CCD system follows a cyclical process in which the RO concentrate is pressurized and recycled back into the RO feed without the need for an ERD. The use of CCD in seawater desalination is characterized by a low SEC of 1.9–2.2 kWh/m^3. However, the permeate obtained from seawater with a TDS

Table 2
Classification of the four main RO configurations based on features, SEC, and product quality.

Category	Configuration	Features	SEC	Product quality	Patent	Reference
Single	Single pass (single stage)	● Most common configuration ● Simple and easy to operate	Standard[a]	Standard[d]	[36]	
	Pressure center	● Improved pump efficiency ● Flexible in operation	Lower[b]			[25]
Pass	Partial pass	● Product quality control for moderate TDS	Higher[c]	Higher[e]	[37]	[26,27]
	SPSP	● Effective TDS reduction for purer product ● Compact BWRO size			[38]	[27,28]
	Multipass	● UPW production			[39]	[29]
Stage	Multistage	● High recovery in BWRO process	Lower[b]	Lower[f]	[40]	[1,30,31]
	CCD	● Circulation of concentrate to RO feed ● Entropic loss due to mixing			[41–43]	[32]
	Batch	● Circulation of unpressurized concentrate to RO feed ● Minimized entropic loss with a batch system			[44]	[23,24]
Inner	ISD	● Arrangement of different RO membranes in a PV ● Uniform flux distribution			[45]	[33–35]

SPSP: split partial second pass. CCD: closed circuit desalination. ISD: internally staged design. TDS: total dissolved solids. BWRO: brackish water reverse osmosis. UPW: ultrapure water. PV: pressure vessel. SEC: specific energy consumption.
[a] The SEC for single-pass RO is defined as the standard.
[b] The SEC is lower than that for single pass.
[c] The SEC is higher than that for single pass.
[d] The TDS of single-pass product is defined as the standard.
[e] The TDS of product is lower than that of single pass.
[f] The TDS of product is higher than that of single pass.

concentration of 35,000 mg/L has a relatively high TDS concentration of 379–682 mg/L [32]. Similar to CCD, the re-circulation of RO concentrate is implemented in a batch system. The main benefit of batch RO is that it requires lower minimum energy due to the similar concentrations of feed to brine resulting in less entropy generation [23,24].

Representative inner RO designs include an internally staged design (ISD) (or a hybrid RO membrane inter-stage design [HID]). In a PV, the flux of the front elements is high and that of rear elements is low. By placing a high-rejection membrane at the head of the PV and a high-flux membrane at the tail, a uniform flux distribution can be achieved inside the PV. This requires lower hydraulic pressure, thus reducing SEC and extending the lifetime of the membranes. The benefits of ISD designs have been investigated in several studies [33–35]. However, product quality tends to be lower because of the high-flux membranes at the rear, which produce a large volume of water from the concentrated feed.

Given that the four main RO design types have their own particular strengths and weaknesses, a combination of these could be employed to optimize RO design for particular purposes. Advances in RO configuration are ongoing. In general, new RO designs are first proposed in patents and their performance analyzed using simulations. Lab-scale or pilot-scale experiments then typically follow to validate the simulation results. Likewise, SSP RO has been applied for a patent and its performance is then validated by simulation.

3. Methods

3.1. Comparison of RO configurations

As discussed in the previous section, pass RO designs produce a high-purity permeate. The newly proposed SSP RO design was compared with existing pass RO designs for SWRO plants to prove its effectiveness in reducing the TDS levels of the permeate and reducing energy costs. Fig. 3 presents the RO configurations that are to be compared. A single pass is depicted in Fig. 3(a). The SSP design in Fig. 3(b) splits the permeate stream, with that taken from the rear of the PV recirculated back into the feed. Fig. 3(c) to (e) represents the SPSP, partial two pass, and two pass, respectively. In this study, SPSP RO split the permeate between the 4th and 5th elements. For partial two-pass RO, it was assumed that 50% of the first-pass RO permeate was bypassed to the final product. The concentrate derived from BWRO was circulated into the SWRO feed in the two-pass RO designs (Fig. 3c to e).

3.2. RO process modeling

In this study, MATLAB (MathWorks R2015a) was employed to model the performance of RO systems in a steady state with a feed containing 35,000 mg/L of TDS at a temperature of 25 °C. The average flux of SWRO elements in a PV was set conservatively at 12.81 L/m^2 h which is close to the typical operating flux of 13–14 L/m^2 h for SWRO plants [46]. An SWRO plant of 100,000 m^3/d capacity with 1250 PVs was considered and a PV containing seven identical RO elements was employed. Recovery Y was set at 40% for SWRO and 80% for BWRO to represent typical operating conditions [23]. To determine the operating hydraulic pressure, the golden section method (GSM) was used in computer code with MATLAB for efficient convergence.

Fig. 4 presents the flow diagram used to evaluate SSP RO performance. Because SSP RO re-circulates the stream from the rear elements back to the RO feed, an additional step was added to the module-scale RO algorithm to calculate the dilution of the RO feed. The constant volume of RO feed was maintained to avoid overload of RO elements. The performance of other RO systems was evaluated with modified algorithms for each.

3.3. Module-scale RO analysis

One of the key factors in determining RO performance is the specifications of the RO membrane modules. The geometries of commercial 8-inch SWRO membrane modules and their performance in typical SWRO test conditions are available from their respective manufacturers. However, the water permeability coefficient A and salt permeability coefficient B are not available online. In this study, the SWRO and BWRO membranes SW30HRLE-400i and BW30-400 were selected [47] and their A and B values calculated for the simulation. The calculated A and B values of SW30HRLE-400i were 1.25 L/m^2 h bar and 5.82×10^{-5} m/h, respectively, and those of BW30-400 were 3.29 L/m^2 h bar and 1.92×10^{-4} m/h, respectively.

Membrane properties are affected by temperature T [°C] so the temperature correction factor TCF [−] in Eq. (1) was employed. The ratio between membrane activation energy e [J/mol] and the universal

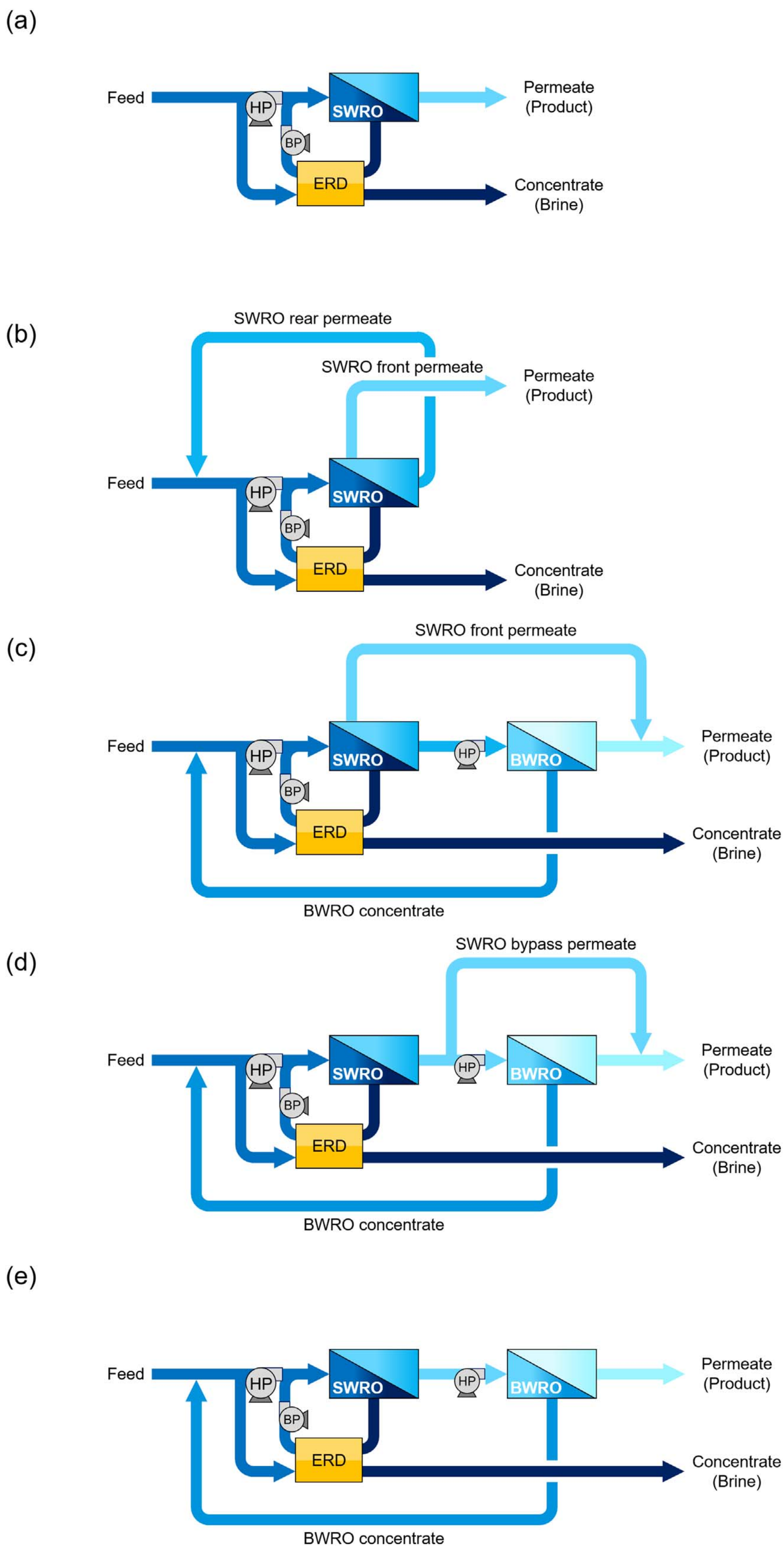

Fig. 3. RO configurations for high-purity permeate production: (a) single pass, (b) SSP, (c) SPSP, (d) partial two pass and (e) two pass. (a) and (b) are RO systems with a single pass, and (c) to (e) are RO systems with two passes.

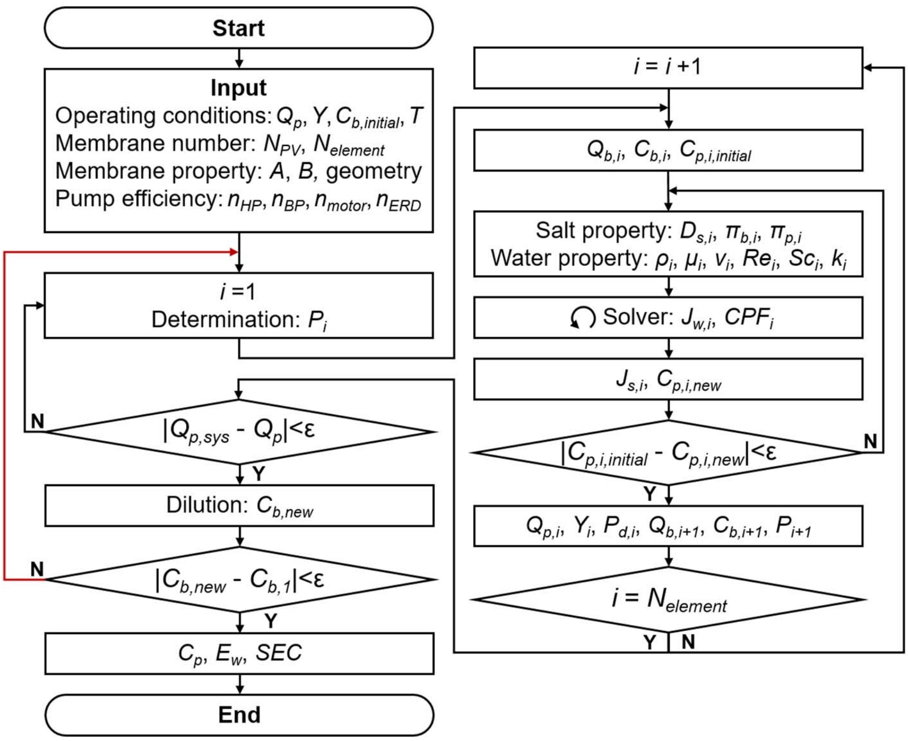

Fig. 4. Flow diagram of the modeling algorithm for the SSP RO process.

gas constant R [J/K mol], e/R [K], was assumed to be 2640 for $T > 25$ °C and 3020 otherwise [48].

$$TCF = \exp\left[\frac{e}{R}\left(\frac{1}{298} - \frac{1}{273 + T}\right)\right] \tag{1}$$

The density ρ of water is affected by temperature and salt concentration. In this study, ρ was assumed to be 1000 kg/m^3, but temperature and salinity were not considered. Viscosity μ [kg/m s] is affected by solute concentration C [mg/L] and T, and it can be expressed by Eq. (2) [28]:

$$\mu = (1.476 \times 10^{-3} + 2.482 \times 10^{-9}C + 9.329 \times 10^{-15}C^2)\exp(-2.008 \times 10^{-2}T) \tag{2}$$

Although various salts are dissolved in actual seawater, it was assumed that the solute in this simulation was composed of sodium chloride with a molecular weight M_w of 58.44 g/mol to simplify the calculation of solute properties. Salt diffusivity D_s [m^2/s] can also be calculated from C and T (Eq. (3)) [28]. Osmotic pressure π [bar] can be expressed by the Van't Hoff equation and the coefficient γ was taken to be 2 in Eq. (4).

$$D_s = 6.725 \times 10^{-6}\exp\left(1.546 \times 10^{-7}C - \frac{2513}{T + 273}\right) \tag{3}$$

$$\pi = \frac{\gamma CR(T + 273) \times 10^{-5}}{M_W} \tag{4}$$

The geometry of the membrane module determines the hydraulic conditions. The cross-flow velocity v [m/s] was calculated from the bulk flow rate Q_b [m^3/d] and total channel area using channel height h [m], width w [m] and the number of channels n [−] in Eq. (5) [49]. Hydraulic diameter d_H [m] in Eq. (6) was calculated from the membrane module geometry.

$$v = \frac{1}{86400}\frac{Q_b}{whn} \tag{5}$$

$$d_H = \frac{2wh}{w + h} \tag{6}$$

The Reynolds number Re [−] and the Schmidt number Sc [−] were expressed using Eqs. (7)–(8) and several of the parameters calculated above. The mass transfer coefficient k [m/s] was calculated from the relationship between the Sherwood Sh [−], Reynolds, and Schmidt numbers (Eqs. (9)–(10)) [23].

$$Re = \frac{\rho v d_H}{\mu} \tag{7}$$

$$Sc = \frac{\mu}{\rho D_s} \tag{8}$$

$$Sh = 0.16Re^{0.605}Sc^{0.42} \tag{9}$$

$$k = Sh\left(\frac{D_s}{d_H}\right) = \frac{0.16Re^{0.605}Sc^{0.42}D_s}{d_H} \tag{10}$$

The governing equations in Eqs. (11)–(12) were solved simultaneously to determine the hydraulic pressure required for achieving a certain RO recovery. As a module-scale model, the equations were integrated over the module length until the constraints such as total module area and the amount of product were met [23]. In the equations, J_w [L/m^2 h] is water flux and J_s [mg/m^2 h] is solute flux. A_m [m^2] is the effective area of the membrane and C_b [mg/L] is the bulk concentration.

$$\frac{dQ_b}{dA_m} = -\frac{24}{1000}J_w \tag{11}$$

$$\frac{dQ_bC_b}{dA_m} = -\frac{24}{1000}J_s \tag{12}$$

To integrate the equations above, water flux and solute flux were calculated with the consideration of concentration polarization factor CPF [−] using Eqs. (13)–(14) [23]. C_m [mg/L] and C_p [mg/L] are the solution concentration at the membrane surface and of the permeate, respectively. Flow factor (FF) was not considered in this study. Rejection in Eq. (15) is indicated by Rej [−]. Because CPF is associated with J_w in Eq. (16), the simultaneous equations were solved using a numerical solver. The initial C_p value was updated with new J_w and J_s values using Eq. (17). Pressure drop P_d along the element length Δz [m]

is expressed in Eq. (18), and the friction factor correction parameter K $[-]$ was determined to be 2.4 [50].

$$J_w = A \times TCF\left[(P_b - P_p) - (CPF \times \pi_b - \pi_p)\right] \quad (13)$$

$$J_s = B \times TCF(CPF \times C_b - C_p) \times 10^3 \quad (14)$$

$$Rej = 1 - \frac{C_p}{C_b} \quad (15)$$

$$CPF = \frac{C_m}{C_b} = \exp\left(\frac{J_w}{k} \times \frac{1}{3.6 \times 10^6}\right)Rej + 1 - Rej \quad (16)$$

$$C_p = \frac{J_s}{J_w} \quad (17)$$

$$P_d = -\frac{\Delta z}{2}\frac{6.23K\rho}{d_H}\left(\frac{Re_i^{-0.3}v_i^2}{2} + \frac{Re_{i+1}^{-0.3}v_{i+1}^2}{2}\right) \times 10^{-5} \quad (18)$$

The efficiency of the HP η_{HP} $[-]$ and BP η_{BP} $[-]$ were taken to be 80% and 60%, respectively. The efficiency of the electric motor η_{motor} $[-]$ and the ERD η_{ERD} $[-]$ were set at 98% and 95%, respectively. For the ERD, it was assumed that pressure is exchanged without a deterioration in feed quality. Energy consumption E_w [kWh/d] was calculated from the feed flow rate $Q_{f,device}$ [m^3/d] and the pressure applied ΔP_{device} [bar] for each device. The calculation takes into consideration the efficiency of each device η_{device} $[-]$ (Eq. (19)). SEC was calculated by dividing E_w by the total permeate produced from the RO system, $Q_{p,sys}$ [m^3/d] (Eq. (20)).

$$E_w = \frac{1}{36}\sum\frac{\Delta P_{device}Q_{f,device}}{\eta_{device}} \quad (19)$$

$$SEC = \frac{E_w}{Q_{p,sys}} \quad (20)$$

3.4. Cost analysis

A cost analysis was performed using several cost functions. Eqs. (21)–(24) were used to calculate capital expenditure (CAPEX) [$/yr]. CC_{SWIP}, CC_{Pump}, CC_{ERD} and CC_m are the capital cost (CC) functions for seawater intake and pretreatment (SWIP), the pump, the ERD and the membrane, respectively [28]. Q_c [m^3/d] in Eq. (23) represents the SWRO concentrate. CC_{total} was expressed as the sum of these CC functions multiplied by the coefficient 1.411 to represent indirect costs (Eq. (25)) [51].

$$CC_{SWIP} = 996(24Q_{f,device})^{0.8} \quad (21)$$

$$CC_{Pump} = 52(\Delta P_{device}Q_{f,device})^{0.8} \quad (22)$$

$$CC_{ERD} = 3134.7Q_c^{0.8} \quad (23)$$

$$CC_m = \sum CC_{element} + \sum CC_{PV} \quad (24)$$

$$CC_{total} = 1.411(CC_{SWIP} + CC_{Pump} + CC_{ERD} + CC_m) \quad (25)$$

Operating expenditure (OPEX) [$/yr] was calculated using Eqs. (26)–(31). OC_m, OC_e, OC_{insure}, OC_{labor}, OC_{ch}, OC_{main} are the operation cost (OC) functions for membrane replacement, energy, insurance, annual labor, chemical supply, and maintenance. Electricity cost C_e [$/kWh] and RO plant load factor f_c $[-]$ were assumed to be 0.08 and 0.9, respectively. OC_{total} was calculated as the sum of the individual OC functions (Eq. (32)) [28].

$$OC_m = 0.2CC_m \quad (26)$$

$$OC_e = 365C_ef_cE_w \quad (27)$$

$$OC_{insure} = 0.005CC_{total} \quad (28)$$

$$OC_{labor} = 0.01 \times 365Q_{p,sys}f_c \quad (29)$$

$$OC_{ch} = 0.0225 \times 365Q_{p,sys}f_c \quad (30)$$

$$OC_{main} = 0.01 \times 365Q_{p,sys}f_c \quad (31)$$

$$OC_{total} = OC_m + OC_e + OC_{insure} + OC_{labor} + OC_{ch} + OC_{main} \quad (32)$$

With an interest rate Ir $[-]$ of 8% and plant operation lifetime y of 25 years, the unit product cost (UPC) [$/m^3] can be calculated by combining the CC_{total} and OC_{total} (Eq. (33)) [28].

$$UPC = \frac{1}{365Q_{p,sys}}\left[CC_{total}\frac{Ir(1+Ir)^y}{(1+Ir)^y - 1} + OC_{total}\right] \quad (33)$$

4. Results and discussion

4.1. Analysis of SSP RO design

In SSP RO, the feed is diluted with permeate from the rear element (s). The more permeate that is blended with the feed, the more diluted the feed becomes. Therefore, it is important to determine the optimal split ratio for SSP RO to achieve target SEC and product quality. For practical SSP RO operation, the characteristics of SSP RO were examined in relation to the split ratio, which ranged from SSP 7 (only permeate from the 7th element is blended with the feed) to SSP 4–7 (permeate from elements 4 through 7 is blended with the feed). The effects on osmotic dilution, flux distribution, energy requirements, and energy consumption were analyzed thoroughly and systematically.

4.1.1. Osmotic dilution and flux distribution

The performance of SSP RO was influenced by the number of split elements because the permeate from the split elements leads to the osmotic dilution of the feed. The feed (TDS concentration = 35,000 mg/L) had an initial osmotic pressure of 29.68 bars, which dropped to 29.15 bars (TDS concentration = 34,375 mg/L) and 25.44 bars (TDS concentration = 30,000 mg/L) when an SSP 7 and an SSP 4–7 split were employed (Fig. 5a). Due to the lower osmotic pressure, the hydraulic pressure required to achieve the water recovery target also fell from 53.43 bars to 52.64 bars and to 47.15 bars for these particular split ratios. The association between energy consumption and applied pressure will be discussed later.

With greater osmotic dilution, the rate of increase in osmotic pressure decreased along the PV. In Fig. 5(a), the osmotic pressure of the feed increased by 3.51 bars between each of the first five elements during regular single-pass RO operation (i.e., no split). In contrast, when the SSP 4–7 split was employed, this increase was only 2.86 bars. This slower increase in osmotic pressure resulted in a more even flux distribution inside the PV (Fig. 5b). The standard deviation of the flux was 7.60 for single-pass RO and 6.66 for SSP 4–7. This means that the difference between the hydraulic pressure and the osmotic pressure along the PV was more even when the feed was diluted. Therefore, the RO elements can produce a more uniform water flux along the PV with the use of SSP RO.

This uniform flux distribution is beneficial in RO operation for a number of reasons. For example, the RO elements are more evenly employed; with the rear elements able to produce more water, the burden on the front elements is lessened. Another benefit is that fouling can be mitigated, particularly in the front elements due to the lowered flux [52,53]. In addition, scaling in the rear elements can be reduced due to the diluted feed concentration [1]. All of these advantages mean that the RO elements in SSP RO can have a longer operational lifetime due to the more even water flux by feed dilution.

4.1.2. Energy requirements for SSP RO

Because the average osmotic pressure decreased with an increase in

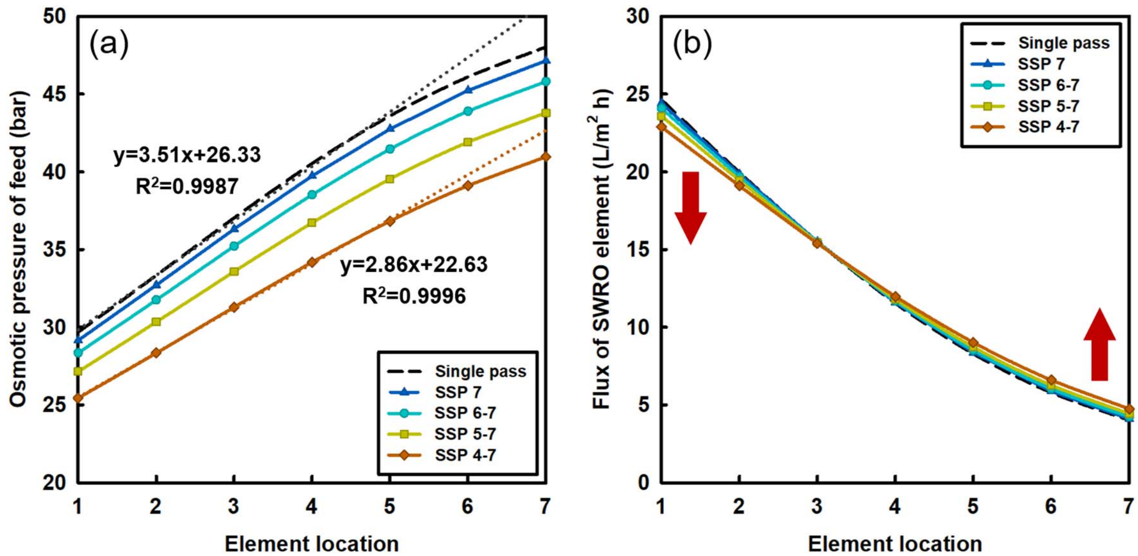

Fig. 5. (a) Osmotic pressure of the feed and (b) the flux distribution of the elements in the PV depending on the split ratio in SSP RO. The data for each configuration were obtained under basic SWRO operating conditions: feed TDS concentration of 35,000 mg/L at 25 °C with a 40% SWRO recovery rate. SSP 7 = SSP RO in which the permeate from the 7th element is blended with the feed. SSP 4–7: the permeate from the 4th and 7th elements is blended with the feed.

the number of elements used for the split, the hydraulic pressure required to generate the target water volume across the PV also decreased. This means that SSP RO has the potential to consume less energy than single-pass RO. However, the SEC of SSP RO was higher than that of single-pass RO due to the loss of rear permeate through circulation. It is thermodynamically obvious that more energy is required to obtain a purer permeate. However, SSP RO needs to consume less SEC than two-pass RO designs if it has a chance to displace these RO configurations for use in SWRO plants. Therefore, it is important that the SEC of SSP RO is lower than that of two-pass RO designs.

Under basic operating conditions, single-pass RO consumed 2.11 kWh/m^3 while the two-pass RO designs required 2.22–2.71 kWh/m^3. In other words, SSP RO is feasible if its SEC ranges between 2.11 and 2.22 kWh/m^3. The SSP 7 split ratio used 2.17 kWh/m^3, which falls within this target range. However, the SEC of SSP 6–7 to SSP 4–7 did not fall within this range. In summary, the split element ratio for SSP RO can be selected to meet the target water quality, but the general application of SSP RO is only economically feasible when the permeate from the 7th element is blended with the feed (Fig. 6).

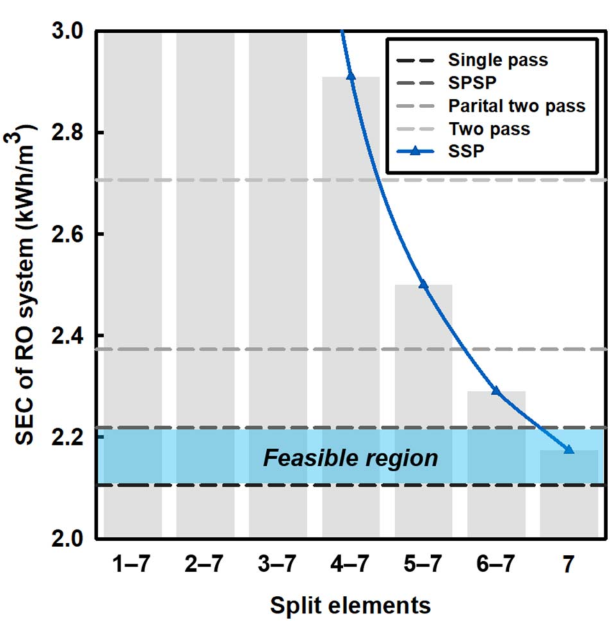

Fig. 6. Energy requirement for the SSP RO design based on SEC for different split ratios.

As discussed in Section 2.1, entropy is generated when solutions with different concentrations are mixed. In most SWRO plants that have adopted second-pass RO, the final BWRO concentrate is circulated into the feed for SWRO, leading to a loss of energy in the BWRO concentrate. However, the energy loss is not included in this study. In other words, two-pass RO configurations require more energy than indicated by the calculated SECs. On the other hand, the SSP RO design inherently minimizes energy loss due to low energy to recover in SWRO permeate, which means a split ratio of SSP 6–7 may also be economically feasible if entropic loss in practice for two-pass ROs is considered.

4.1.3. Energy consumption of SSP 7 RO

SSP 7 is the most appropriate SSP RO design in terms of minimizing energy consumption compared to the two-pass RO designs. The SEC for SSP 7 varies in accordance with the feed characteristics, as with other RO configurations. Of the various feed parameters, salinity and temperature are critical factors that determine the amount of energy required during operation.

SSP RO required less energy when the feed had a lower TDS concentration (Fig. 7a). At 40% SWRO recovery, SSP 7 used 1.94 kWh/m^3 when the TDS concentration of the feed was 30,000 mg/L, rising to 2.42 kWh/m^3 for a TDS concentration of 40,000 mg/L. Optimal recovery decreased when the salinity of the feed increased. This is related to the more rapid increase in osmotic pressure at high TDS concentrations. When the feed has high initial salinity, it becomes more rapidly concentrated after the permeate is extracted and its osmotic pressure reaches the hydraulic pressure. This means a high recovery rate accelerates feed enrichment; thus, the optimal recovery level decreases with increasing feed salinity. The maximum recovery for SSP 7 was observed to be 48% for the feed with a TDS concentration of 40,000 mg/L; in contrast, feeds of 30,000 mg/L and 35,000 mg/L were able to reach recovery rates of 50%.

The membrane properties *A* and *B* increased with increasing temperature. At a recovery rate of 40%, SSP 7 consumed 2.24 kWh/m^3 when the feed solution was 20 °C and 2.11 kWh/m^3 at 35 °C. Higher temperatures also reduced the SEC and decreased the optimal recovery rate of the SSP RO process. This was also due to the concentrated feed more rapidly increasing the osmotic pressure. At temperatures of 20 °C and 25 °C, SSP 7 obtained a recovery rate of 50%; however, SSP 7 could

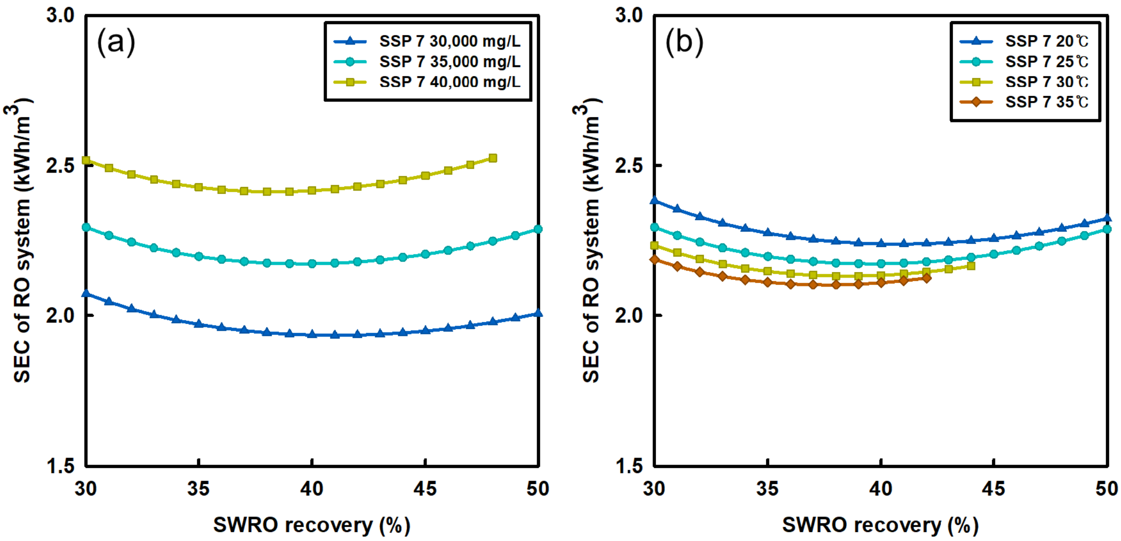

Fig. 7. SEC of SSP 7 depending on (a) feed salinity at 25 °C and (b) temperature with a feed TDS concentration of 35,000 mg/L.

not achieve a recovery rate over 45% when the temperature of the feed was higher than 30 °C using the membrane selected for this study. In summary, high temperatures reduced the energy consumption of SSP 7 but limited its recovery rate (Fig. 7b).

4.2. Performance of the RO systems

In Section 4.1, it was discovered that the use of SSP RO is practical when the permeate split occurs between the 6th and 7th elements (i.e., SSP 7). To compare the performance of SSP RO with other RO configurations, the product quality and SEC were analyzed under various settings for SWRO recovery, feed quality, and temperature.

4.2.1. Product quality

It is crucial to analyze the product quality of an RO system to meet water standards. SWRO recovery, feed quality, and temperature affect the product of RO systems; they all reduce permeate water quality when they increase.

Fig. 8(a) displays permeate quality in relation to SWRO recovery rate. Single-pass RO produced a permeate with a TDS concentration of between 200 and 261 mg/L, while that of SSP 7 RO had a TDS concentration of between 177 and 219 mg/L. When feed salinity varied, the TDS concentration of single-pass RO permeate had a range of 190–271 mg/L and SSP 7 RO had a range of 163–232 mg/L (Fig. 8b). An increase in temperature also increased permeate TDS levels for single-pass RO (187–301 mg/L) and SSP 7 RO (161–257 mg/L; Fig. 8c). Overall, SSP 7 RO produced a permeate that was approximately 15% purer than single-pass RO.

With the growing need for high-quality water, stringent water standards such as low TDS (i.e., TDS < 200 mg/L) and low concentration of some species are required for desalinated water. Depending on the operating conditions and membranes to use, SSP 7 RO can meet these standards by producing purer permeate without needing to adopt second-pass RO. In this case, SSP 7 RO is the single-pass RO process that still meets the stricter desalination water standards.

4.2.2. Specific energy consumption

With the improvement in water quality, SSP 7 was also more energy-efficient than two-pass ROs. For all SWRO recovery rates (30–50%), the SEC of SSP 7 RO was higher than that of single-pass RO (Fig. 9a), which ranged from 2.10 to 2.26 kWh/m^3 and had an optimal recovery rate of 37%. SSP 7 RO consumed 2.17 to 2.29 kWh/m^3 with an optimal recovery rate of 40%. Importantly, however, this SEC was lower than that of the two-pass RO designs for all recovery rates. In fact, the SEC for two-pass ROs was 2.20 to 2.40 kWh/m^3 for SPSP, 2.37 to 2.51 kWh/m^3 for partial two pass, and 2.71 to 2.83 kWh/m^3 for two pass. Overall, the SEC of single-pass RO and that of SSP RO became

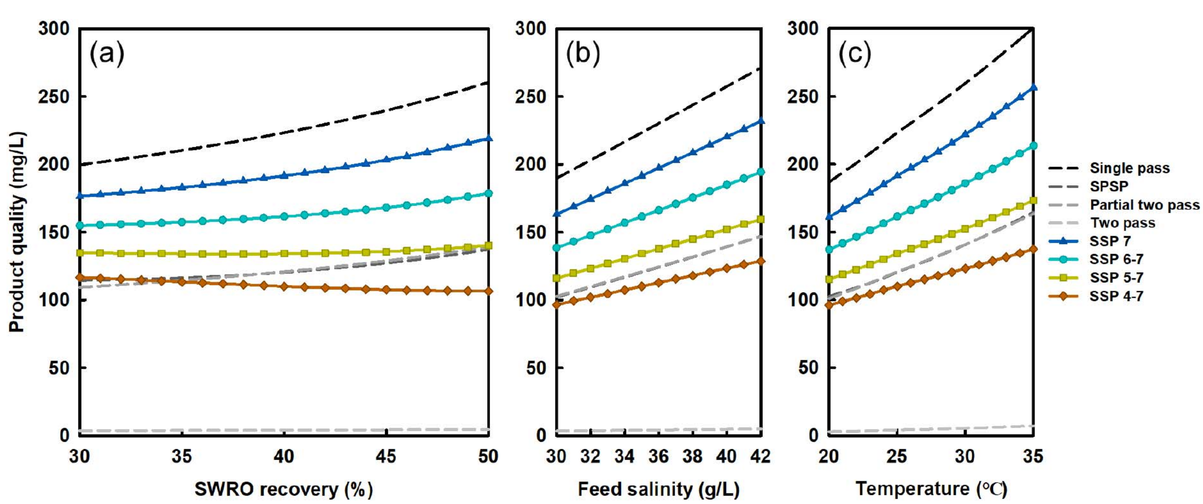

Fig. 8. Product quality of different RO systems under various operating conditions: (a) SWRO recovery, (b) feed salinity, and (c) temperature.

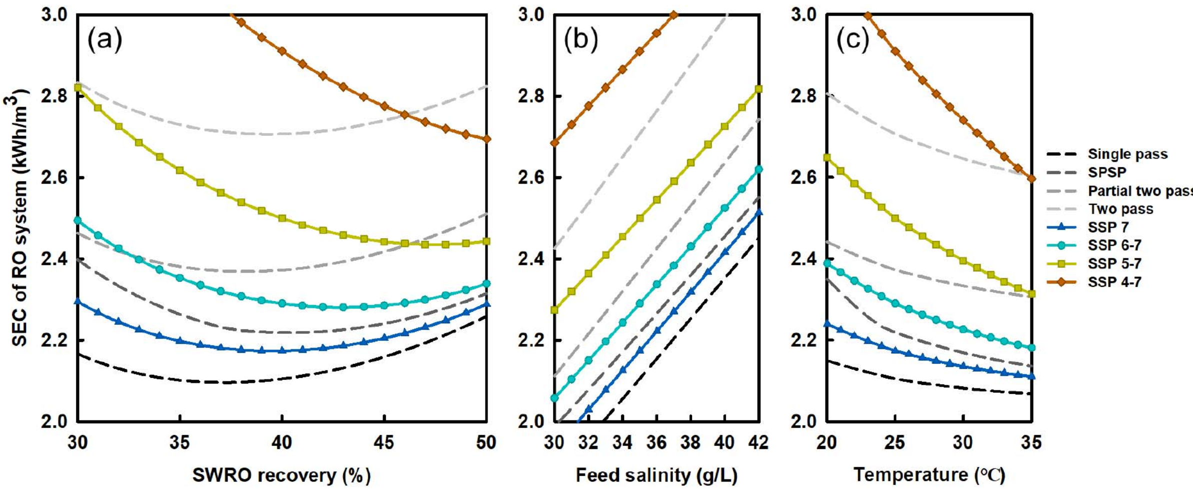

Fig. 9. SEC for different RO systems under various operating conditions: (a) SWRO recovery, (b) feed salinity, and (c) temperature.

more similar as the recovery rate increased, with the difference in SEC ranging from 0.13 to 0.03 kWh/m^3.

Similar results were obtained for variation in feed quality (Fig. 9b). SSP 7 RO had a lower SEC than did the two-pass RO designs but this was higher than that of the single-pass RO design. The increase in feed salinity increased energy requirements; the SEC for SSP 7 RO changed from 1.94 to 2.51 kWh/m^3 when the feed salinity changed from 30,000 to 42,000 mg/L. The SEC for the single-pass and SPSP RO designs ranged between 1.86 and 2.45 kWh/m^3 and 1.99 and 2.55 kWh/m^3, respectively.

Fig. 9(c) shows that feed temperature affected the energy consumption of SSP 7 RO, with higher temperatures reducing the SEC (2.24 kWh/m^3 for 20 °C and 2.11 kWh/m^3 for 35 °C). The single-pass and SPSP RO designs also followed the same trend (2.15–2.07 kWh/m^3 and 2.35–2.14 kWh/m^3, respectively). Overall, SSP 7 RO exhibited a lower SEC than did the two-pass RO designs for all operating conditions, but this was higher than that of single-pass RO. Thus, the SSP RO offers an option to improve final water quality without compromising energy efficiency over two-pass ROs. Considering the SEC of two-pass ROs may be underpredicted as mentioned in Section 4.1.2, the benefit of SSP RO in energy saving would be increased further.

4.3. Analysis of specific energy consumption

SSP 7 RO exhibited a higher SEC than that of single-pass RO but lower than that of the two-pass RO designs. The relationship between SEC and RO configuration was analyzed by separating SEC into its constituent parts (i.e., the energy requirements for the SWRO HP, SWRO BP, and BWRO HP). Fig. 10(a) shows that the SWRO HP was the most energy intensive device for all RO configurations. Originally, 4.64 kWh/m^3 was required to operate single-pass RO. However, the use of ERDs dramatically reduced the SEC of RO systems. The total SEC for single-pass RO was 2.11 kWh/m^3 with the application of an ERD. In particular, 1.86 kWh/m^3 was consumed by the HP for the SWRO feed and the remaining 0.25 kWh/m^3 was used by the BP for SWRO feed pressurized by the ERD. In SSP RO, a diluted feed was used in SWRO and its overall energy consumption was lower than that for single-pass RO. However, SEC is defined as the energy consumption divided by product amount and thus the SEC of SSP 7 RO increases due to the lower volume of final product. For the two-pass RO designs, BWRO was adopted to produce a purer product. BWRO not only used more energy but also generated concentrate, leading to the loss of final product. For these reasons, the SEC of the two-pass RO designs was higher than that of the single-pass RO designs.

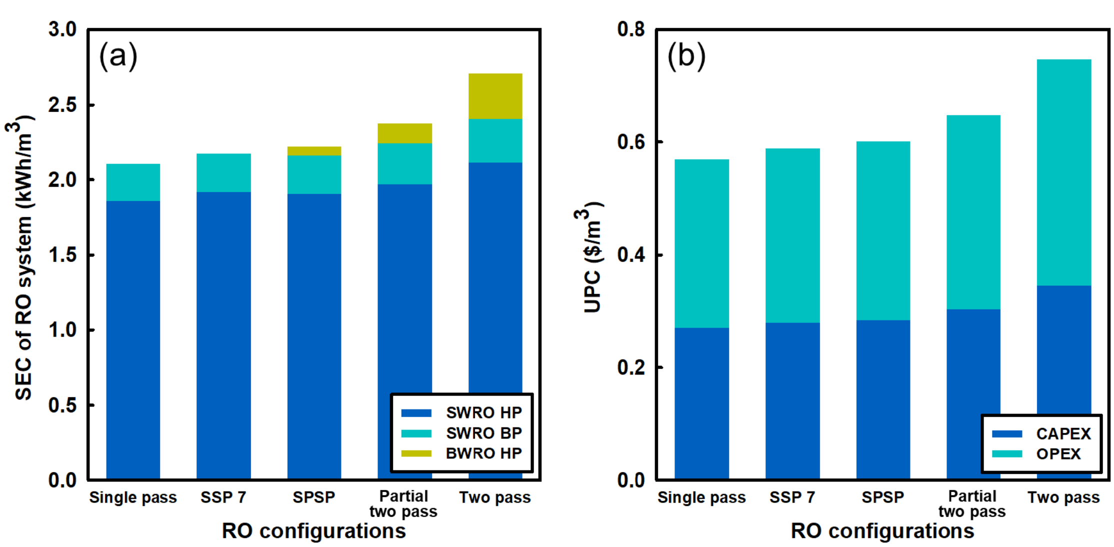

Fig. 10. (a) SEC and (b) UPC breakdown for different RO configurations.

4.4. Analysis of unit product cost

Economic benefits were also investigated in Fig. 10(b) by calculating the UPC. The shapes of Fig. 10(a) and (b) look similar, illustrating that UPC and SEC were connected. The UPC for single-pass RO designs was 0.569 $/m^3 for single pass and 0.588 $/m^3 for SSP 7. On the other hand, the two-pass RO designs were subject to the additional cost of operating BWRO (including CAPEX and OPEX). The UPC for the two-pass designs was 0.601 $/m^3 for SPSP, 0.648 $/m^3 for partial two pass, and 0.747 $/m^3 for two pass. Section 4.1.1 explains that less fouling will occur in the SSP 7 RO process due to the uniform flux distribution and the diluted feed. Thus, operation can continue over a longer time period compared to single-pass RO, leading to lowered OC. In addition, as explained in Section 4.1.2, the actual SEC of two-pass ROs is higher than the calculated value, resulting in the increase of UPC for two-pass ROs. In summary, SSP 7 RO was more economical than the two-pass RO designs and its UPC is more competitive.

5. Conclusions

In this study, SSP RO was presented for the first time and its performance investigated using computer modeling. SSP RO is a single-pass RO design that produces high-purity permeate due to the dilution of the SWRO feed with permeate from the rear of the PV. This dilution leads to a relatively uniform flux distribution and a lower fouling propensity, resulting in longer-term SWRO operation. Also, SSP RO required less hydraulic pressure due to the diluted SWRO feed. In terms of split ratio, SSP RO is economically feasible compared to the two-pass RO configurations when the permeate from the 7th element is blended with the SWRO feed.

The main benefit of SSP RO is to produce purer permeate. SSP RO can satisfy stricter water standards, which is not achievable by conventional single-pass RO. In addition, SSP RO has advantages as a single-pass configuration where BWRO operation is not required. Therefore, SSP 7 RO consumed less energy than the two-pass RO designs under all of the tested operating conditions. It was further characterized by relatively low water production costs (i.e., UPC) compared to the designs using second-pass RO.

The practical application of SSP has not yet been investigated, but the possibility of application has been discussed. With major benefits to its design, it is expected that SWRO desalination plants that adopt SSP RO would be installed. In addition, the fact that SSP RO can function with a single PV facilitates the application of the design; for example, it can be employed in small desalination plants in which second-pass RO operation is not feasible. In an era of water scarcity, SSP RO is a promising new technology that can both improve water quality and reduce energy expenditure.

Acknowledgement

This work is supported by a Korea Agency for Infrastructure Technology Advancement (KAIA) grant funded by the Ministry of Land, Infrastructure and Transport (Grant 17IFIP-B116952-02).

References

[1] S. Lin, M. Elimelech, Staged reverse osmosis operation: Configurations, energy efficiency, and application potential, Desalination 366 (2015) 9–14.
[2] Reverse osmosis: membranes help beat the drought, Filtr. Sep. 46 (2009) 23–24.
[3] A. Efraty, Closed circuit desalination series no-6: conventional RO compared with the conceptually different new closed circuit desalination technology, Desalin. Water Treat. 41 (2012) 279–295.
[4] Veolia Water Technologies, Sadara, Veolia Water Technologies, 2017, https://www.veoliawatertechnologies.com/en/media/articles/sadara , Accessed date: 28 October 2017.
[5] M.A. Sanza, V. Bonnélyea, G. Cremerb, Fujairah reverse osmosis plant: 2 years of operation, Desalination 203 (2007) 91–99.
[6] R. Einav, K. Harussi, D. Perry, The footprint of the desalination processes on the environment, Desalination 152 (2003) 141–154.
[7] V.G. Gude, Energy consumption and recovery in reverse osmosis, Desalin. Water Treat. 36 (2011) 239–260.
[8] D.I. Kim, J. Kim, H.K. Shon, S. Hong, Pressure retarded osmosis (PRO) for integrating seawater desalination and wastewater reclamation: energy consumption and fouling, J. Membr. Sci. 483 (2015) 34–41.
[9] B. Peñate, L. García-Rodríguez, Current trends and future prospects in the design of seawater reverse osmosis desalination technology, Desalination 284 (2012) 1–8.
[10] N. Ghaffour, J. Bundschuh, H. Mahmoudi, M.F. Goosen, Renewable energy-driven desalination technologies: a comprehensive review on challenges and potential applications of integrated systems, Desalination 356 (2015) 94–114.
[11] J.R. Werber, C.O. Osuji, M. Elimelech, Materials for next-generation desalination and water purification membranes, Nat. Rev. Mater. 1 (2016) 16018.
[12] J.R. Werber, A. Deshmukh, M. Elimelech, The critical need for increased selectivity, not increased water permeability, for desalination membranes, Environ. Sci. Technol. Lett. 3 (2016) 112–120.
[13] SUEZ Australia & New Zealand, Perth Seawater Desalination Plant, SUEZ Water Australia (n.d.). http://www.degremont.com.au/media/Perth_Seawater_Desalination_Plant_1.pdf (accessed 10/28/2017).
[14] R. Singh, Membrane Technology and Engineering for Water Purification: Application, Systems Design and Operation, Butterworth-Heinemann, 2014.
[15] M. Faigon, Y. Egozy, D. Hefer, M. Ilevicky, Y. Pinhas, Hadera desalination plant two years of operation, Desalin. Water Treat. 51 (2013) 132–139.
[16] G. Schneier-Madanes, M.-F. Courel, Water and sustainability in arid regions, in: G. Zehtabian, H. Khosravi, M. Ghodsi (Eds.), High Demand in a Land of Water Scarcity: Iran, 13 Springer, London, New York, 2010, pp. 75–86.
[17] B. Sauvet-Goichon, Ashkelon desalination plant—a successful challenge, Desalination 203 (2007) 75–81.
[18] A. Hermony, I. Sutzkover-Gutman, Y. Talmi, O. Fine, Palmachim seawater desalination plant—seven years of expansions with uninterrupted operation together with process improvements, Desalin. Water Treat. 55 (2015) 2526–2535.
[19] Y. Hanegbi, Y. Mansdorf, Status of palmachim desalination project, Program and Papers of 8th Annual Conference, Proceedings of the Innovations and Applications of Sea-Water and Marginal Water Desalination, Israel Desalination Society, Israel, 2006, pp. 11–16.
[20] A. Yechiel, Y. Shevah, Optimization of energy costs for SWRO desalination plants, Desalin. Water Treat. 46 (2012) 304–311.
[21] A. Cipollina, G. Micale, L. Rizzuti, Seawater Desalination: Conventional and Renewable Energy Processes, Springer Science & Business Media (2009).
[22] C. Huttche, R. Orquiza, Y.P. Lelean, Pollution Control Study for Tuas Desalination and Power Plant Project, (2011).
[23] J.R. Werber, A. Deshmukh, M. Elimelech, Can batch or semi-batch processes save energy in reverse-osmosis desalination? Desalination 402 (2017) 109–122.
[24] D.M. Warsinger, E.W. Tow, K.G. Nayar, L.A. Maswadeh, Energy efficiency of batch and semi-batch (CCRO) reverse osmosis desalination, Water Res. 106 (2016) 272–282.
[25] N. Voutchkov, Seawater desalination—costs and technology trends, Encyclopedia of Membrane Science and Technology, Wiley, 2013, , http://dx.doi.org/10.1002/9781118522318.emst115.
[26] M. Wilf, C. Bartels, Optimization of seawater RO systems design, Desalination 173 (2005) 1–12.
[27] S. Rybar, R. Boda, C. Bartels, Split partial second pass design for SWRO plants, Desalin. Water Treat. 13 (2010) 186–194.
[28] Y. Du, L. Xie, Y. Liu, S. Zhang, Y. Xu, Optimization of reverse osmosis networks with split partial second pass design, Desalination 365 (2015) 365–380.
[29] H. Lee, Y. Jin, S. Hong, Recent transitions in ultrapure water (UPW) technology: Rising role of reverse osmosis (RO), Desalination 399 (2016) 185–197.
[30] M. Li, Reducing specific energy consumption in reverse osmosis (RO) water desalination: an analysis from first principles, Desalination 276 (2011) 128–135.
[31] M. Elimelech, W.A. Phillip, The future of seawater desalination: energy, technology, and the environment, Science 333 (2011) 712–717.
[32] Z. Gal, A. Efraty, CCD series no. 18: record low energy in closed-circuit desalination of ocean seawater with nanoH_2O elements without ERD, Desalin. Water Treat. 57 (2016) 9180–9189.
[33] V.G. Molina, M. Busch, P. Sehn, Cost savings by novel seawater reverse osmosis elements and design concepts, Desalin. Water Treat. 7 (2009) 160–177.
[34] V.G. Molina, A. Casañas, Reverse osmosis, a key technology in combating water scarcity in Spain, Desalination 250 (2010) 950–955.
[35] B. Peñate, L. García-Rodríguez, Reverse osmosis hybrid membrane inter-stage design: a comparative performance assessment, Desalination 281 (2011) 354–363.
[36] G.A. Pittner, Reverse osmosis system, Google Patents, 1986.
[37] H.S. Kim, Y.K. Oh, S.H. Park, Y.G. Park, Two-pass reverse osmosis desalination apparatus and method, Google Patents, 2012.
[38] D.T. Bray, Simultaneous production of multiple grades of purified water by reverse osmosis, Google Patents, 1977.
[39] A.A. Tonelli, A. Deutschmann, S.L. Wesno, High purity water using triple pass reverse osmosis (TPRO), Google Patents, 2000.
[40] H. Yamamura, M. Kurihara, K. Maeda, Apparatus and method for multistage reverse osmosis separation, Google Patents, 2001.
[41] A. Efraty, Continuous closed-circuit desalination apparatus without containers, Google Patents, 2010.
[42] L. Szucz, A. Szucs, Method and apparatus for treating fluids containing foreign materials by membrane filter equipment, Google Patents, 1991.
[43] R.I. Bratt, Method and apparatus for fluid treatment by reverse osmosis, Google Patents, 1989.
[44] A. Efraty, Apparatus for continuous closed circuit desalination under variable

pressure with a single container, Google Patents, 2009.

[45] H. Husain, P. Cote, F. Kent, Nanofiltration system for water softening with internally staged spiral wound modules, Google Patents, 2004.

[46] A. Efraty, R.N. Barak, Z. Gal, Closed circuit desalination series no-2: new affordable technology for sea water desalination of low energy and high flux using short modules without need of energy recovery, Desalin. Water Treat. 42 (2012) 189–196.

[47] The Dow Chemical Company, Reverse Osmosis & Nanofiltration Types, The Dow Chemical Company (n.d.). http://www.dow.com/en-us/water-and-process-solutions/products/reverse-osmosis (accessed 10/28/2017).

[48] Dow Water & Process Solutions, FILMTEC™ Reverse Osmosis Membranes Technical Manual, The Dow Chemical Company (n.d.). http://msdssearch.dow.com/PublishedLiteratureDOWCOM/dh_095b/0901b8038095b91d.pdf?filepath=/609-00071.pdf&fromPage=GetDoc (accessed 10/28/2017).

[49] L. Song, S. Hong, J. Hu, S. Ong, W. Ng, Simulations of full-scale reverse osmosis membrane process, J. Environ. Eng. 128 (2002) 960–966.

[50] V. Geraldes, N.E. Pereira, M. Norberta de Pinho, Simulation and optimization of medium-sized seawater reverse osmosis processes with spiral-wound modules, Ind. Eng. Chem. Res. 44 (2005) 1897–1905.

[51] A. Malek, M. Hawlader, J. Ho, Design and economics of RO seawater desalination, Desalination 105 (1996) 245–261.

[52] T. Chong, F. Wong, A. Fane, The effect of imposed flux on biofouling in reverse osmosis: role of concentration polarisation and biofilm enhanced osmotic pressure phenomena, J. Membr. Sci. 325 (2008) 840–850.

[53] C.Y. Tang, T. Chong, A.G. Fane, Colloidal interactions and fouling of NF and RO membranes: a review, Adv. Colloid Interf. Sci. 164 (2011) 126–143.